Geomechanics and Engineering, *Vol. 37, No. 1 (2024) 1-8*
https://doi.org/10.12989/gae.2024.37.1.001

An analytical solution for buckling failure of rock slopes based on elastoplastic slab theory

Zhihong Zhang[1], Pengyu Wu[1], Fuchu Dai[1], Renjiang Li*[2], Xiaoming Zhao[2] and Shu Jiang[2]

[1]*Key Laboratory of Urban Security and Disaster Engineering of the Ministry of Education, Beijing University of Technology, Beijing 100124, China*
[2]*China Three Gorges Corporation, Wuhan 430010, China*

(*Received May 5, 2023, Revised February 29, 2024, Accepted March 2, 2024*)

Abstract. Buckling failure is one of the classical types of catastrophic landslides developing on inclination-paralleled rock slopes, which is mainly governed by its self-weight, earthquake and ground water. However, nearly none of the existing studies fully consider the influence of slope self-weight, earthquake and ground water on the mechanical model of buckling failure. In this paper, based on energy equilibrium principle and elastoplastic slab theory, a thorough mechanical analysis on bucking slopes has been carried out. Furthermore, an analytical solution for slip bucking failure of rock slopes has been proposed, which fully considers the effect of slope self-weight, seismic force and hydrostatic pressure. Finally, the methodology is used to conduct comparative analysis with other analytical solutions for three practical buckling studies. The results show that the proposed approach is capable of providing a more accurate and reasonable evaluation for stability of rock slopes with potential buckling failure.

Keywords: analytical solution; buckling failure; elastoplastic slab theory; slope stability

1. Introduction

As a special gravitational landslide, buckling failure in the inclination-paralleled rock slopes often occurs with catastrophic destruction (Cavers 1981). In recent decades, taking the Qinghai-Tibet Plateau as an example, the number of bucking failure slopes has increased significantly with the frequent occurrence of extreme climate (He *et al*. 2021), such as the Tangjiashan landslide, Donghekou landslide, Wenjiagou landslide and Xiaguiwa landslide (Wang *et al*. 2009, Wang *et al*. 2014, Zhang *et al*. 2016, Li *et al*. 2021, Zhang *et al*. 2022). These large-scale buckling failures have caused great economic loss and brought threat for human lives or property. Therefore, a lot of studies have been conducted to understand the bucking failure mechanism. The buckling deformation is a kind of creep deformation caused by the slope's self-weight (Radbruch-Hall 1978). Meanwhile, external factors such as earthquake, rainfall and ground water can also trigger or accelerate the slope failure. According to the phenomenon of actual deformation observed, the process of buckling failure can be divided into three phases, namely, moderate deformed phase, heavy deformed phase and failure phase (Pan *et al*. 1990, Ren *et al*. 1998, Zhao *et al*. 2018, Li *et al*. 2018, Khalfi *et al*. 2020, Zhang *et al*. 2022, Wang *et al*. 2022)

Due to the suddenness, complexity and destructiveness of buckling landslides, a number of investigations focused on the mechanical mechanism, furthermore, proposed the criteria for the buckling failure of rock slope. Generally, the slope is simplified to be an elastic beam or elastic slab. According to the regular bending characteristics of rock beam/slab, two regular mechanical models are the Euler buckling failure model and three hinged buckling failure model (Cavers 1981, Hu *et al*. 1993). Using the stability theory for elastic beam and energy equilibrium principle, the critical buckling length of rock slab was determined (Ren *et al*. 1998, Liu *et al*. 2014) as follows.

$$l_{\mathrm{cr}} = h\left\{\frac{n\pi^2 E}{6[n\gamma h\sin\alpha - (n\gamma h\cos\alpha\cdot\tan\varphi + c)]}\right\}^{\frac{1}{3}} \quad (1)$$

where l_{cr} is the critical buckling length, h is the thickness of buckled rock stratum, n is the layer number of rock stratum, E is the elastic modulus of rock, γ is the unit weight of rock, α is the dip angle of rock, c is the cohesion and φ is the friction angle. Considering the influence of lateral force, Liu (1997) proposed a calculation method for the critical buckling length based on Euler buckling failure model for elastic beam. However, it is worth noting that there are significant differences between Euler buckling failure model and actual failure model. Consequently, dividing the slope length into the active segments and the passive segments, the Euler buckling failure model has been improved by the three-hinge buckling model (Garzon 2016). Cavers (1981) and Zhang *et al*. (2019) proposed a calculation method for the critical buckling length based on the three-hinge buckling failure model, which is as follows

*Corresponding author, Senior Engineer
E-mail: li_renjiang@ctg.com.cn

ISSN: 2005-307X (Print), 2092-6219 (Online)

$$l_{\mathrm{cr}}=\left[\frac{\pi^2 Eh^2}{2.25(\gamma\sin\alpha-\gamma\cos\alpha\tan\varphi-c/h)}\right]^{\frac{1}{3}} \tag{2}$$

It can be seen that the above models have not considered the external environmental factors such as external loading, earthquake, and groundwater. Therefore, Liu *et al*. (2016) considered the effect of the top loading on the slope critical buckling height. Following the elastic beam theory, Xiao *et al*. (2014) proposed a calculation method for critical buckling length based on the three-hinge buckling failure model, considering the combined effect of the self-weight of rock slope, the earthquake and the groundwater. Qi *et al*. (2014), Ding and Hu (2020) thought that when the rock stratum was buckled, the uplift height perpendicular to the rock stratum approached infinity. Under this assumption, a three-hinge buckling failure model was established in which the influences of the self-weight of rock, earthquake and ground water were considered. Furthermore, a calculation method for the critical buckling length has been proposed, which is as follows

$$\begin{aligned}&2G(L-l_{\mathrm{cr}})(k_2+\frac{l_{\mathrm{cr}}}{2(L-l_{\mathrm{cr}})}k_2+k_1\tan\varphi)\\&=\frac{8\pi^2}{l_{\mathrm{cr}}^{\,2}}EI+2c(L-l_{\mathrm{cr}})+2G(L-l_{\mathrm{cr}})\sin\alpha(\frac{\tan\varphi}{\tan\alpha}-1)-\gamma_w(l_1-l_{\mathrm{cr}})^2\sin\alpha\tan\varphi-l_{\mathrm{cr}}G\sin\alpha\end{aligned} \tag{3}$$

where L is total length of slope; G is the intensity of gravitational load; l_1 is the distance from the bottom of the slope to the groundwater table along the x direction ; k_1 and k_2 are the component of the seismic coefficient in the normal and parallel direction to the beam; γ_w is the unit weight of water.

For the inclination-paralleled rock slopes, due to various natural geological processes, the slope is divided into many discontinuities and can be viewed as a rock slab with limited length. Liu *et al*. (2002) established a three-hinge buckling failure model and proposed a calculation method for critical buckling length through regarding the rock slope as a three-dimensional compression slab, which is as follows

$$\begin{aligned}&\frac{\pi^2 D}{b^4}l_{\mathrm{cr}}^4+\left[\frac{\gamma h}{2}\sin\alpha-\gamma h(\sin\alpha-\cos\alpha\tan\varphi)+c\right]l_{\mathrm{cr}}^3\\&+\left\{\frac{2\pi^2 D}{b^2}-L\left[\gamma h(\sin\alpha-\cos\alpha\tan\varphi)-c\right]\right\}l_{\mathrm{cr}}^2+\pi^2 D=0\end{aligned} \tag{4}$$

where b is the width of slope; D is the bending stiffness of slab of unit width; μ is the Poisson's ratio.

It should be pointed out that the rock masses were treated as elastic materials (beams or slabs) in the above models. Since the rock masses with buckling deformation exceeded elastic limit before buckling, the simplification of the elastic material failed to express the actual buckling process. Therefore, Feng *et al*. (2010) introduced the plastic reduction factor and established a three-hinge buckling failure model viewing the rock stratum as an elastoplastic slab. Finally, a calculation method for the critical buckling length was proposed, which is as follows

$$\begin{aligned}&\frac{\pi^2 D}{b^4}l_{\mathrm{cr}}^4+\left[\gamma h(\sin\alpha-\cos\alpha\tan\varphi)-c-\frac{\gamma h}{2}\sin\alpha\right]l_{\mathrm{cr}}^3\\&+\left\{\frac{2\pi^2 D\sqrt{\psi_t}}{b^2}-L\left[\gamma h(\sin\alpha-\cos\alpha\tan\varphi)-c-\frac{\gamma h}{2}\sin\alpha\right]\right\}l_{\mathrm{cr}}^2+\pi^2 D\psi_t=0\end{aligned} \tag{5}$$

where ψ_t is the plasticity reduction factor.

As discussed above, for the buckling failure model, none of the existing research considered the combined influence of slope self-weight, seismic force and hydrostatic pressure based on the elastoplastic theory. Meanwhile, it is not rational that the rock material is assumed to be an elastic beam or slab in the practical slope engineering. Therefore, based on energy equilibrium principle and elastoplastic slab theory, this study focuses on proposing an analytical solution for buckling failure of rock slopes considering the effect of slope self-weight, earthquake and ground water, which provides a good understanding about the deformation mechanism of rock slopes.

2. Mechanical model for buckling failure

2.1 Assumptions

In general, the rock stratum thickness of inclination-paralleled rock slopes is far less than its length and width, so the rock slope is assumed to be an elastoplastic thin slab in this investigation.

Main assumptions are as follows:

(1) Rock masses slip along the direction of slope length.

(2) The bottom of passive segment is simplified as a restrain of hinge support, and its periphery is simplified as a roller bearing.

(3) The buckling deformation is a small deformation.

2.2 Mechanical analysis of buckling failure

Based on the above assumptions, a mechanical model for inclination-paralleled rock slope is shown in Fig. 1, in which L is the slope length, b is the slope width, h is the thickness of rock stratum, and α is the rock dip angle. Under the combined actions of slope self-weight G, seismic force S and hydrostatic pressure F_{w}, the buckling deformation of slope occurs. In this study, the whole slope length is divided

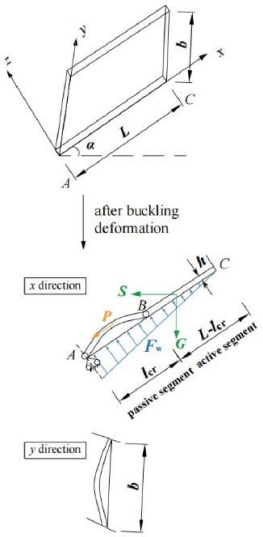

Fig. 1 Mechanical schematic diagram of rock stratum

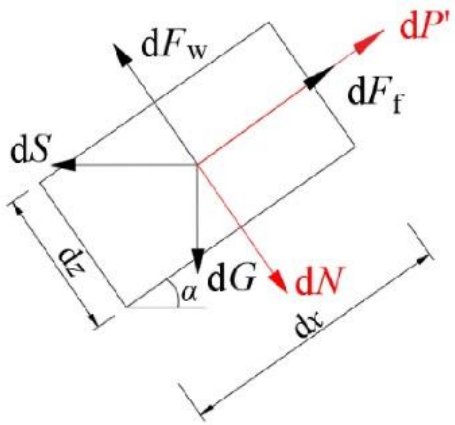

Fig. 2 Two-dimensional mechanical schematic diagram of the unit of active segment

into two segments, the passive segment (or bending segment) AB and active segment (or slipping segment) BC, which are expressed by l_{cr} and L-l_{cr}, respectively.

According to Newton's third law of motion, the propulsive force of active segment to passive segment (P) is equal to the force of the passive segment to the active segment (P') along x direction. In order to determine the propulsive force (P), the active segment (BC) is chosen as the research object for mechanical analysis, see Fig. 2. F_f is the interlayer friction force and N is the normal force.

The self-weight of active segment (dG) can be expressed as

$$\mathrm{d}G = \gamma h \mathrm{d}x\mathrm{d}y \tag{6}$$

where γ is the unit weight of the rock slab and h is the thickness of rock slab.

Here, the impact of ground water is considered, that is, the maximum water level coincides with the surface of slope. Then the hydrostatic pressure (dF_w) of active segment can be expressed as

$$\mathrm{d}F_w = \gamma_w (L - x')\sin\alpha \mathrm{d}y\mathrm{d}z \tag{7}$$

where γ_w is the unit weight of water and x' is the distance along x direction.

The effect of earthquake is described by the seismic inertial force (dS) as

$$\mathrm{d}S = \beta_s K_s \gamma h \mathrm{d}x\mathrm{d}y \tag{8}$$

where β_s is the dynamic magnification factor and K_s is the seismic coefficient.

The normal force (dN) acted on the active segment and interlayer friction force (dF_f) can be expressed as

$$\mathrm{d}N = \mathrm{d}G\cos\alpha - \mathrm{d}S\sin\alpha - \mathrm{d}F_w \tag{9}$$

$$\mathrm{d}F_f = c + \mathrm{d}N\tan\varphi \tag{10}$$

where φ is the friction angle of interface between the rock slab and its underlying rock slab.

Finally, the force of passive segment to the active segment force along x direction (P') can be expressed as

$$\begin{aligned} P' &= \int_{l_\alpha}^{L}\int_0^b \mathrm{d}G\sin\alpha\mathrm{d}x\mathrm{d}y + \int_{l_\alpha}^{L}\int_0^b \mathrm{d}s\cos\alpha\mathrm{d}x\mathrm{d}y - \int_{l_\alpha}^{L}\int_0^b \mathrm{d}F_f\mathrm{d}x\mathrm{d}y \\ &= (L - l_{cx})b\left[\gamma h(\sin\alpha - \tan\varphi) + \beta_s K_s \gamma h(\cos\alpha + \sin\alpha\tan\varphi) - c\right] \\ &\quad + \frac{1}{2}\gamma_w b(L - l_{cr})^2 \sin\alpha\tan\varphi \end{aligned} \tag{11}$$

For simplicity, setting $Q = \gamma h(\sin\alpha - \cos\alpha\tan\varphi) + \beta_s K_s \gamma h(\cos\alpha + \sin\alpha\tan\varphi) - c$, then Eq. (11) can be written as

$$P' = (L - l_{cr})Qb + \frac{1}{2}\gamma_w b(L - l_{cr})^2 \sin\alpha\tan\varphi \tag{12}$$

According to Newton's third law of motion, the propulsive force of the active segment to the passive segment (P) is equal to the force of the passive segment to the active segment P' along x direction. Then

$$P = P' = (L - l_{cr})Qb + \frac{1}{2}\gamma_w b(L - l_{cr})^2 \sin\alpha\tan\varphi \tag{13}$$

2.3 Buckling deformation analysis

According to the theory of thin slab, the critical bending stress is the smallest when there is only one half-wave in the compression direction (y). Therefore, the flexure deformation equation of rock slab on passive segment can be defined as (Liu 1997, Feng *et al*. 2010)

$$w = f\sin\frac{\pi x}{l_{cr}}\cdot\sin\frac{\pi y}{b} \tag{14}$$

where w is the deflection of rock slab and f is the maximum deflection of rock slab on passive segment.

Meanwhile, Eq. (14) satisfies the following conditions

$$\begin{cases} w(x = 0, x = l_{cr}) = 0 \\ w(y = 0, y = b) = 0 \\ \dfrac{\partial^2 w}{\partial x^2}(x = 0, x = l_{cr}) = 0 \\ \dfrac{\partial^2 w}{\partial y^2}(y = 0, y = b) = 0 \end{cases} \tag{15}$$

Therefore, the maximum deflection yields.

$$w_{\max} = w(x = \frac{l_{cr}}{2}, y = \frac{b}{2}) = f\sin\frac{\pi}{l_{cr}}\frac{l_{cr}}{2}\sin\frac{\pi}{b}\frac{b}{2} = f \tag{16}$$

3. Judgement method for buckling failure

During the process from buckling deformation to failure, the total work produced by self-weight and external force is equal to the deformation energy produced by bending deformation of rock mass (Wang 2005). Based on energy equilibrium principle, a judgement method of buckling failure for rock slope is established.

3.1 Energy variation during buckling failure

3.1.1 Work calculation

In this section, a mechanical analysis for the unit body of passive segment is carried out. According to the theory for thin slab (Liu *et al*. 2016), the self-weight of rock stratum along *y* direction and *z* direction can be omitted. Therefore, the surface force N_x on the passive segment along *x* direction can be expressed as

$$N_x = \int_0^{l_{cr}} \int_0^b \mathrm{d}G \sin\alpha \mathrm{d}x\mathrm{d}y + \int_0^{l_{cr}} \int_0^b \mathrm{d}S \cos\alpha \mathrm{d}x\mathrm{d}y - \int_0^{l_{cr}} \int_0^b \mathrm{d}F_f \mathrm{d}x\mathrm{d}y \quad (17)$$

The work produced by self-gravity of rock stratum and the external forces can be expressed as

$$\Delta W = N_x \cdot \mathrm{d}\Delta \quad (18)$$

where $\mathrm{d}\Delta$ is the interlayer displacement along x direction, which can be described by (Liu *et al*. 2016)

$$\mathrm{d}\Delta = \sqrt{1+(\frac{\partial w}{\partial x})^2} - 1 = \frac{1}{2}(\frac{\partial w}{\partial x})^2 \mathrm{d}x \quad (19)$$

Substituting Eq. (19) into Eq. (18) yields

$$\Delta W = \frac{1}{2}\int_0^b N_x \left[\int_0^{l_{cr}} \left(\frac{\partial w}{\partial x}\right)^2 \mathrm{d}x\right]\mathrm{d}y \quad (20)$$

Finally, substituting Eqs. (14) and (17) into Eq. (20) yields

$$\begin{aligned}\Delta W &= \frac{1}{2}\int_0^b N_x \left[\int_0^{l_{cr}} (\frac{\pi^2}{l_{cr}^2} f^2 \cos^2\frac{\pi x}{l_{cr}} \sin^2\frac{\pi y}{b})\mathrm{d}x\right]\mathrm{d}y \\ &= \frac{h}{2}\int_0^b \left[\frac{(L-l_{cr})Q+\frac{1}{2}\gamma_w(L-l_{cr})^2\sin\alpha\tan\varphi}{h} + \gamma(l_{cr}-x)\cdot(\sin\alpha+\beta_s K_s\cos\alpha)\right] \\ &\quad \cdot \left[\int_0^{l_{cr}} \left(\frac{\pi^2}{l_{cr}^2} f^2 \cos^2\frac{\pi x}{l_{cr}} \sin^2\frac{\pi y}{b}\right)\mathrm{d}x\right]\mathrm{d}y \\ &= \frac{\pi^2\left[\frac{(L-l_{cr})Q+\frac{1}{2}\gamma_w(L-l_{cr})^2\sin\alpha\tan\varphi}{h}\right]bh}{8l_{cr}} f^2 + \frac{\pi^2\gamma bh(\sin\alpha+\beta_s K_s\cos\alpha)}{16} f^2\end{aligned} \quad (21)$$

For simplicity, setting $\xi = \dfrac{(L-l_{cr})Q+\frac{1}{2}\gamma_w(L-l_{cr})^2\sin\alpha\tan\varphi}{h}$, then Eq. (21) can be written as

$$\Delta W = \frac{\pi^2\xi bh}{8l_{cr}} f^2 + \frac{\pi^2\gamma bh(\sin\alpha+\beta_s K_s\cos\alpha)}{16} f^2 \quad (22)$$

3.1.2 Deformation potential energy

Since the elastic limit of rock has been exceed before buckling failure, the rock stratum is always regarded as elastoplastic material. In this study, the plastic reduction coefficient ψ_t has been introduced to reflect the influence of plastic deformation on rock mechanical properties. ψ_t is expressed as (Liu *et al*. 2002, Feng *et al*. 2010)

$$\psi_t = E_t / E \quad (23)$$

where E_t is the tangent modulus and E is the elastic modulus.

Here, the rock material is viewed as anisotropic elastoplastic slab. In *x* direction, because the bending stress of the rock layer exceeds its elastic limit, the material modulus E_x becomes the tangent modulus E_t, namely $E_x = E_t = \psi_t E$. In *y* direction, the elastic modulus of rock mass remains unchanged, namely $E_y = E$. For the Poisson's ratio μ, in the process of buckling deformation, it is considered to be constant, namely $\mu_{xy} = \mu_{yx} = \mu$. In x direction, bending stiffness D_x can be written as

$$D_x = \psi_t D = \frac{\psi_t E h^3}{12(1-\mu^2)} = \frac{E_t h^3}{12(1-\mu^2)} \quad (24)$$

where D is the bending stiffness of slab per unit width.

In *y* direction, the bending stiffness D_y remains unchanged, namely $D_y = D$.

For the torsional stiffness D_k of rock slab, it can be written as

$$D_k = \frac{G' h^3}{12} = \frac{\sqrt{\psi_t} E h^3}{24(1+\mu)} = \frac{1-\mu}{2}\cdot\sqrt{\psi_t} D \quad (25)$$

where G' is the elastic shear modulus, and can be written as

$$G' = \frac{\sqrt{\psi_t} E}{2(1+\mu)} \quad (26)$$

Then the variation of deformation potential energy ΔU of passive segment can be expressed as

$$\Delta U = \frac{1}{2}\int_0^{l_{cr}} \int_0^b \left[D_x\left(\frac{\partial^2 w}{\partial x^2}\right)^2 + D_y\left(\frac{\partial^2 w}{\partial y^2}\right)^2 + 2D_x\mu\frac{\partial^2 w}{\partial x^2}\frac{\partial^2 w}{\partial y^2} + 4D_k\left(\frac{\partial^2 w}{\partial x \partial y}\right)^2\right]\mathrm{d}x\,\mathrm{d}y \quad (27)$$

Substituting Eq. (14) into Eq. (27), the variation of the deformation potential energy ΔU of the passive segment can be obtained as

$$\begin{aligned}\Delta U &= \frac{D}{2} f^2 \left[\int_0^{l_{cr}} \int_0^b (\psi_t \frac{\pi^4}{l_{cr}^4} + 2\psi_t\mu\frac{\pi^4}{l_{cr}^2 b^2} + \frac{\pi^4}{b^4})\sin^2\frac{\pi x}{l_{cr}}\sin^2\frac{\pi y}{b} + 2(1-\mu)\sqrt{\psi_t}\frac{\pi^4}{l_{cr}^2 b^2}\cos^2\frac{\pi x}{l_{cr}}\cos^2\frac{\pi y}{b}\right]\mathrm{d}x\mathrm{d}y \\ &= \frac{D}{2} f^2 \left[\psi_t \frac{\pi^4}{l_{cr}^4} + 2\psi_t\mu\frac{\pi^4}{l_{cr}^2 b^2} + \frac{\pi^4}{b^4} + 2(1-\mu)\sqrt{\psi_t}\frac{\pi^4}{l_{cr}^2 b^2}\right]\frac{l_{cr} b}{4} \\ &= \frac{l_{cr} b D}{8}[\psi_t \frac{\pi^4}{l_{cr}^4} + 2\psi_t\mu\frac{\pi^4}{l_{cr}^2 b^2} + \frac{\pi^4}{b^4} + 2(1-\mu)\sqrt{\psi_t}\frac{\pi^4}{l_{cr}^2 b^2}] f^2\end{aligned} \quad (28)$$

3.2 Stability factor

According to the energy equilibrium principle, in the process from buckling deformation to buckling failure, the variation of deformation potential energy stored by the buckling deformation should be equal to the total work produced by the self-weight, earthquake and groundwater, which means

$$\Delta W = \Delta U \quad (29)$$

Substituting Eqs. (22) and (28) into Eq. (29) yields

$$[\xi + \frac{\gamma l_{cr}(\sin\alpha+\beta_s K_s\cos\alpha)}{2}] - \frac{\pi^2 D}{hb^2}[\psi_t \frac{b^2}{l_{cr}^2} + 2\psi_t\mu + \frac{l_{cr}^2}{b^2} + 2(1-\mu)\sqrt{\psi_t}] = 0 \quad (30)$$

Based on Eq. (30), the critical buckling length l_{cr} can be calculated by

$$\left(\frac{\pi^2 D}{b^4}-\frac{1}{2}\gamma_w \sin\alpha\tan\varphi\right)l_{cr}^4+\left(Q+\gamma_w L\sin\alpha\tan\varphi-\frac{\gamma h(\sin\alpha+\beta_s K_s\cos\alpha)}{2}\right)l_{cr}^3$$
$$+\left\{\frac{\pi^2 D}{b^2}[2\mu\psi_t+2(1-\mu)\sqrt{\psi_t}]-LQ-\frac{1}{2}\gamma_w L^2\sin\alpha\tan\varphi\right\}l_{cr}^2+\pi^2 D\psi_t=0 \quad (31)$$

Accordingly, the sliding stress $\boldsymbol{\sigma}^*$ and the critical stress $\boldsymbol{\sigma}_{\mathbf{cr}}$ can be defined as

$$\sigma^*=\xi+\frac{\gamma l_{cr}(\sin\alpha+\beta_s K_s\cos\alpha)}{2}$$
$$=\frac{(L-l_{cr})Q+\frac{1}{2}\gamma_w(L-l_{cr})^2\sin\alpha\tan\varphi}{h}+\frac{\gamma l_{cr}(\sin\alpha+\beta_s K_s\cos\alpha)}{2} \quad (32)$$

$$\sigma_{cr}=\frac{\pi^2 D}{hb^2}\left[\psi_t\frac{b^2}{l_{cr}^2}+2\psi_t\mu+\frac{l_{cr}^2}{b^2}+2(1-\mu)\sqrt{\psi_t}\right] \quad (33)$$

When the sliding force is greater than critical stress, the slope tends to failure. Therefore, the stability factor of rock slope can be defined by

$$K=\frac{\sigma_{cr}}{\sigma^*}=\frac{\frac{\pi^2 D}{hb^2}\left[\psi_t\frac{b^2}{l_{cr}^2}+2\psi_t\mu+\frac{l_{cr}^2}{b^2}+2(1-\mu)\sqrt{\psi_t}\right]}{\frac{(L-l_{cr})Q+\frac{1}{2}\gamma_w(L-l_{cr})^2\sin\alpha\tan\varphi}{h}+\frac{\gamma l_{cr}(\sin\alpha+\beta_s K_s\cos\alpha)}{2}} \quad (34)$$

In conclusion, the proposed analytical solution for buckling failure considers the combined effect of slope self-weight, seismic force and hydrostatic pressure, by viewing the rock slope as an elastoplastic and anisotropic thin slab. It is worth noting that when Eq. (31) does not consider the influence of earthquake and groundwater, it can be degraded to Eq. (5). When Eq. (31) does not consider the influence of plasticity, earthquake and groundwater, it can be degraded to Eq. (4), which indicate that the proposed method can better reflect actual conditions.

3.3 Judgement criteria for buckling failure

In this section, the stability factor of slope K and critical buckling length l_{cr} are chosen to evaluate the slope stability. The critical buckling length can determine the deformation condition of passive segment (or bending segment) by comparing with actual buckling length, and the stability factor can determine the rock slope stability. When the stability factor K is greater than 1, the slope remains stable. Meanwhile, as the critical buckling length l_{cr} is less than actual buckling length l_{ac}, the active segment (or slipping segment) of slope continues movement which means the deformation of passive segment (or bending segment) does not reach the maximum value, thereby the slope remains stable and vice versa. Therefore, to ensure accurate judgement of rock slopes stability with potential buckling failure, the two judgement criteria should be comprehensively adopted. The detailed judgement criteria for buckling failure is shown in Table 1.

Table 1 Judgement criteria for buckling failure

Evaluation index	Condition	Stability
K	$K>1$	Stable
	$K<1$	Unstable
l_{cr}	$l_{cr}>l_{ac}$	Unstable
	$l_{cr}<l_{ac}$	Stable

4. Model validation

Three cases of bucking failure reported in the literatures were chosen to conduct an evaluation of the proposed method for buckling judgement, and comparative analysis were carried out with other existing assessment methods (three-hinge buckling failure model for elastic beam, Euler buckling failure model for elastic beam and three-hinge buckling failure model for elastic beam considering earthquake).

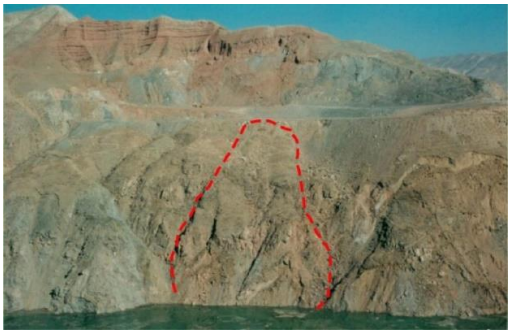

Fig. 3 No.2 landslide of Lijiaxia Hydropower Station

4.1 No. 2 landslide of Lijiaxia Hydropower Station

No. 2 landslide is located at the left bank of upstream of Lijiaxia Hydropower Station, China (Liao 2002), which is a large and deep bedding rock slope with typical buckling failure. It covers an area of 0.255 km^2 and total volume is 1405×10^4 m^3. The width and longitudinal length of landslide is 360 m and 810 m, respectively. Boundary of No. 2 landslide is marked in red in Fig. 3.

The physical and geometric parameters of No.2 landslide of Lijiaxia Hydropower Station are given in Table 2. Using these parameters, the critical buckling length l_{cr} have been calculated by Eqs. (1), (2), (3) and Eq. (31), and what's more, the safety factors have been determined by Eqs. (6), (7) and (34). All the comparative results with different assessment methods (three-hinge buckling failure model for elastic beam, Euler buckling failure model for elastic beam, three-hinge buckling failure model for elastic beam considering earthquake, proposed three-hinge buckling failure model for elastoplastic slab considering slope self-weight, seismic force and hydrostatic pressure) are shown in Table 3.

It can be seen from Table 3 that No.2 slope is unstable because the stability factors calculated by four methods are all less than 1.05, which is with the real scenario in agreement. However, it is worth noting that compared to the actual buckling length, the three existing methods caused the overestimations of critical buckling length due to their negligence on the influence of earthquake and groundwater, but the value of critical buckling length (133 m) obtained by the analytical solution (three-hinge buckling failure model

Table 2 Parameters of No.2 landslide (Liao 2002)

Property	Value
Bedding dip α (°)	45
Total length L (m)	360
Actual buckling length l_{ac} (m)	136
Width of slope b (m)	810
Stratum thickness h (m)	3
Unit weight γ (kN/m^3)	2.7×10^3
Friction angle φ (°)	19
Young's modulus E (GPa)	9
Poison's ratio μ	0.2
Plasticity reduction coefficient ψ_t	1.0

Table 3 Comparative analysis of No.2 landslide with different assessment methods

Calculation method	Buckling length	Stability factor	Stability
Actual condition	136 m	—	unstable
Euler buckling failure model for elastic beam (Ren *et al.* 1998, Liu *et al.* 2014)	220 m	0.61	unstable
Three-hinge buckling failure model for elastic beam (Cavers 1981)	344 m	0.95	unstable
Three-hinge buckling failure model for elastic beam considering earthquake (Qi *et al.* 2014)	304 m	0.73	unstable
Proposed three-hinge buckling failure model for elastoplastic slab	133 m	0.96	unstable

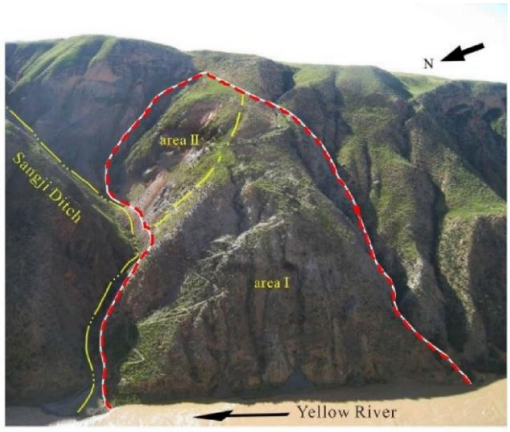

Fig. 4 No.3 landslide of Yellow River Hydropower Station

for elastoplastic slab) is closest to the actual value of critical buckling length (136 m). Therefore, the proposed analytical method provides a favorable support for efficiently evaluating the stability of rock slope using critical buckling length and the safety factor.

4.2 No. 3 landslide of Yellow River Hydropower Station in Cihaxia

No. 3 landslide of Yellow River Hydropower Station in Cihaxia (Li 2019) is located on the right bank of Yellow River, and slate and metamorphic sandstone are the main

Table 4 Physical and mechanical parameters of rock material (Li 2019)

Property	Value
Bedding dip α (°)	60
Total length L (m)	60
Actual buckling length l_{ac} (m)	28
Width of slope b (m)	80
Stratum thickness h (m)	0.2
Unit weight γ (kN/m^3)	2.2×10^3
Friction angle φ (°)	10
Young's modulus E (GPa)	12
Poison's ratio μ	0.3
Plasticity reduction factor ψ_t	1.0

Table 5 Comparative analysis of No.3 landslide with different assessment methods

Calculation method	Buckling length	Stability factor	Stability
Actual condition	28 m	—	unstable
Euler buckling failure model for elastic beam (Ren *et al.* 1998, Liu *et al.* 2014)	35 m	0.60	unstable
Three-hinge buckling failure model for elastic beam (Cavers 1981)	115 m	3.84	stable
Three-hinge buckling failure model for elastic beam considering earthquake (Qi *et al.* 2014)	55 m	0.80	unstable
Proposed three-hinge buckling failure model for elastoplastic slab	25 m	0.86	unstable

lithology. The average attitude is NW343°∠60°, the height is about 300 m. As shown in Fig. 4, the landslide can be divided into area I and area II. Two developing buckling deformations existed in the middle and toe of slope can be found. Here, we choose the middle buckling section as the research object.

Table 4 gives the physical and mechanical parameters of No. 3 landslide. Using these parameters, the critical buckling length l_{cr} have been calculated by Eqs. (1), (2), (3) and (31), and what's more, the safety factors have been determined by Eqs. (6), (7) and (34). All the comparative results with different assessment methods are shown in Table 5.

According to the results in Table 5, No.3 slope is unstable because the stability factors calculated by three methods (Euler buckling failure model for elastic beam, three-hinge buckling failure model for elastic beam considering earthquake, proposed three-hinge buckling failure model for elastoplastic slab) are all less than 1.05, which is consistent with the actual condition. More importantly, the critical buckling length (25 m) calculated by the proposed method is closest to the actual buckling length (28 m), this conclusion is consistent with that in section 4.1, which indicates that the proposed judgement method can reasonably assess No. 3 landslide of Yellow River Hydropower Station in Cihaxia. However, when the three-hinge buckling failure model for

Table 6 Parameters of rock material of Xiaguiwa landslide (Li *et al*. 2021)

Property	Value
Bedding dip α (°)	60
Total length L (m)	875
Buckling deformation length l_{ac} (m)	530
Width of slope b (m)	200
Stratum thickness h (m)	1
Unit weight γ (kN/m^3)	2.2×10^3
Friction angle φ (°)	29
Young's modulus E (GPa)	9.1
Poison's ratio μ	0.25
Plasticity reduction factor ψ_t	1.0

Table 7 Comparative analysis of Xiaguiwa landslide with different assessment methods

Calculation method	Buckling length	Stability factor	Stability
Actual condition	530 m	—	stable
Euler buckling failure model for elastic beam (Ren *et al*. 1998, Liu *et al*. 2014)	268 m	0.31	unstable
Three-hinge buckling failure model for elastic beam (Cavers 1981)	137 m	0.016	unstable
Three-hinge buckling failure model for elastic beam considering earthquake (Qi *et al.* 2014)	226 m	0.93	unstable
Proposed three-hinge buckling failure model for elastoplastic slab	483 m	1.08	stable

elastic beam is applied, the stability of No. 3 slope is stable which is contrary to the actual situation, which should be attributed to the negligence of the influence of earthquake and groundwater. Additionally, when the combined effects of earthquake and groundwater are not considered, the application of Euler buckling failure model for elastic beam and three-hinge buckling failure model for elastic beam considering earthquake can trigger the obvious overestimations of critical buckling length. It is well known that a competitive judging method for slope stability iscrucial to risk assessment and control in slope engineering, Consequently, the proposed analytical solution for buckling failure of rock slope based on theory of elastoplastic slab has very favorable advantage for evaluating slope stability.

4.3 Xiaguiwa landslide

Xiaguiwa landslide (Li *et al*. 2021, Zhang *et al*. 2022) is located at Batang country, left bank of the Jinsha River, southeast fringe of Tibetan Plateau, China. According to the field investigations, the bedrock of Xiaguiwa landslide mainly consists of sandstone interbedded with mica schist. One of the prominent features is that the whole process from deep-seated buckling deformation to failure can be thoroughly observed. In this section, the heavy deformed zone in Fig. 5 is chosen as the study case.

Table 6 gives the physical and mechanical parameters about Xiaguiwa landslide. Same as section 4.1 and 4.2, using parameters in Table 6, the critical buckling length l_{cr} have been calculated by Eqs. (1), (2), (3) and (31), and the safety factors have also been determined by Eqs. (6), (7) and (34). All the comparative results with different assessment methods are shown in Table 7.

It can be seen from Fig.5, the study zone remains stable despite heavy or severe deformation. According to the results in Table 7, only the result obtained by the proposed model is similar to that of the actual situation, which shows the stability of slope is stable. However, we notice other three models obtain the opposite results. Not only the slope is regarded as unstable, but also there are significant differences between calculated values of critical buckling length (268 m, 137 m, 226 m) and actual value (530 m). The negligence of the comprehensive impact of earthquake and groundwater should be responsible for these deviated judgements. When the proposed method considers the combined effect of earthquake and groundwater, it is obvious that the value of critical buckling length (483 m) calculated by the proposed method is closest to the actual value (530 m), which strongly proves the accuracy of proposed analytical solution for buckling failure of rock slope based on theory of elastoplastic slab.

5. Conclusions

• Based on energy equilibrium principle and elastoplastic slab theory, an analytical solution for bucking failure of rock slopes has been proposed, which fully considers the effect of slope self-weight, seismic force and hydrostatic pressure.

• Three applications of real cases indicate that the proposed analytical solution provides a more accurate and reasonable evaluation of stratified rock slopes with potential buckling failure. In some studies, those existing analytical methods based on Euler buckling failure model for elastic beam, three-hinge buckling failure model for elastic beam considering or not earthquake usually overestimate or underestimate the critical buckling length.

• The proposed judgement method for buckling failure of rock slope provides a theoretical basis for predicting buckling failure in practical slopes.

Acknowledgments

This study is financially supported by the Second Tibetan Plateau Scientific Expedition and Research (STEP) Program (No. 2019QZKK0905) and the Scientific Research Project of China Three Gorges Corporation (No. YMJ(BHT)/(21)036).

Conflict of Interest

The authors declare no conflict of interest.

References

Cavers, D.S. (1981), "Simple methods to analyze buckling of rock slopes", *Rock Mech*, **14**(2), 87-104. https://doi.org/10.1007/BF01239857.

Ding, G. and Hu, X. (2020), "Mechanical mechanism of buckling failure of Dabenliu consequent bedding rockslide", *Bull. Geol. Sci. Technol.*, **39**(2), 186-190. https://doi.org//CNKI:SUN:DZKQ.0.2020-02-022.

Feng, J., Zhou, D. and Yang, T. (2010), "Stability analysis of consequent rock slopes using elastic-plastic plate theory", *Chin. J. Geotech. Eng.*, **32**(8), 1184-1188. https://doi.org/CNKI:SUN:YTGC.0.2010-08-009.

Garzon, S.E.R. (2016), "Analytical solution for assessing continuum buckling in sedimentary rock slopes based on the tangent-modulus theory", *Int. J. Rock Mech. Min. Sci.*, **90**, 53-61. https://dx.doi.org/10.1016/j.ijrmms.2016.10.002.

He, J., Qi, S., Zhan, Z., Guo, S., Li, C., Zheng, B., Huang, X., Zou, Y., Yang, G. and Liang, N. (2021), "Seismic response characteristics and deformation evolution of the bedding rock slope using a large-scale shaking table", *Landslides*, **18**(8), 2835-2853. https://doi.org/10.1007/s10346-021-01682-w.

Hu, X. and Cruden, D. (1993), "Buckling deformation in the Highwood Pass, Alberta, Canada", *Can. Geotech. J.*, **30**(2), 276-286. https://doi.org/10.1139/t93-023.

Khalfi, Y., Sofiane, G. and Bouchikhi, A.S. (2020), "A novel refined shear deformation theory for the buckling analysis of thick isotropic and orthotropic plates on two-parameter pasternak's foundations", *J Fail. Anal. Preven.*, **20**, 75-84. https://doi.org/10.1007/s11668-019-00713-y.

Li, X., Chen, H., Sun, Y., Zhou, R. and Wang, L. (2018), "Study on the splitting failure of the surrounding rock of underground caverns", *Geomech. Eng.*, **14**(5), 499-507. https://doi.org/10.12989/gae.2018.14.5.499.

Li, J. (2019), "Layer slabbing effect on deformation and failure in consequent rock slope", Ph.D. Dissertation, Lanzhou University, Lanzhou, China.

Li, Y., Feng, X., Yao, A., Li, S. and Guo, M. (2021), "A massive ancient river-damming landslide triggered by buckling failure in the upper Jinsha River, SE Tibetan Plateau", *Bull. Eng. Geol. Environ.*, **2,** 1-13. https://doi.org/10.1007/s10064-021-02293-4.

Liao, Y. (2002), "Analysis & study on stability of NO.2 landslide for Lijiaxia hydropower station on yellow river", Ph.D. Dissertation, Chengdu University of Technology, Chengdu, China.

Liu, C. and Zhu, Y. (2014), "Buckling failure model of inclination-paralleled rock slopes", *J. Geol. Hazards Environ. Preserv*, **25**(1), 82-86. https://doi.org//10.3969/j.issn.1006-4362.2014.01.015.

Liu, H., Wang, G. and Huang, F. (2016), "Methods to analyze flexural buckling of the consequent slabbed rock slope under top loading", *Math. Probl. Eng.*, 1-8. https://doi.org//10.1155/2016/3402547.

Liu, X. and Zhou, D. (2002), "Stability analysis of layered dip rocky slopes with elastic plane theory", *Rock Soil Mech*, **2**, 162-165. https://doi.org/10.16285/j.rsm.2002.02.007.

Liu, J. (1997), "Calculation method for the buckling problem of inclination-paralleled slopes", *Hydrogeol Eng Geol*, **6**, 37-41. https://doi:10.16030/j.cnki.issn.1000-3665.1997.06.011.

Pan, R., Li, B. and Jiang, J. (1990), "Research on the buckling failure of the slab-rent structure rock bedding slopes", *J Southwest Jiaotong Univ.*, **3**, 82-88.

Qi, S., Lan, H. and Dong, J. (2014), "An analytical solution to slip buckling slope failure triggered by earthquake", *Eng. Geol.*, **194**, 4-11. https://doi.org/10.1016/j.enggeo.2014.06.004.

Radbruch-Hall, D.H. (1978), "Gravitational creep of rock masses on slopes", *Developments in Geotech Eng*, **14**:607-657. https://doi.org/10.1016/B978-0-444-41507-3.50025-8.

Ren, G., Li, S., Nie, D. and Zuo, S. (1998), "The physical simulation and mechanical analysis on landslide's formation mechanism on consequent slope", *Mountain. Res.*, **16**(3), 3-5. https://doi.org/10.16089/j.cnki.1008-2786.1998.03.005.

Wang, F., Cheng, Q., Highland, L., Miyajima, M., Wang, H. and Yan, C. (2009), "Preliminary investigation of some large landslides triggered by the 2008 Wenchuan earthquake, Sichuan Province, China", *Landslides*, **6**, 47-54. https://doi.org/10.1007/s10346-009-0141-z.

Wang, G., Huang, R., Lourenco, S.D.N. and Kamai, T. (2014), "A large landslide triggered by the 2008 Wenchuan (M8.0) earthquake in Donghekou area: phenomena and mechanisms", *Eng. Geol.*, **182**, 148-157. https://doi.org/10.1016/j.enggeo.2014.07.013.

Wang, Q., Zhang, R. and Zheng, H. (2022), "Buckling failure analysis and numerical manifold method simulation for Malvern Hills slope", *Rock Soil Mech.*, **43**(7), 1951-1960. https://doi.org/10.16285/j.rsm.2021.1674.

Xiao, H., Hou, K. and Du, J. (2014), "The study on buckling failure of different layer of layer rock mass slope", *Sci. Technol. Eng.*, **14**(2), 1671-1815. https://doi.org/10.3969/j.issn.1671-1815.2014.02.051.

Zhang, M., Yin, Y. and McSaveney, M. (2016), "Dynamics of the 2008 earthquake-triggered Wenjiagou Creek rock avalanche, Qingping, Sichuan, China", *Eng. Geol.*, **200**, 75-87. https://doi.org/10.1016/j.enggeo.2015.12.008.

Zhang, Q., Hu, J., Gao, Y., Du, Y., Li, L., Liu, H. and Sun, S. (2022), "Analysis of the buckling failure of bedding slope based on monitoring data-a model test study", *Geomech. Eng.*, **28**(4), 335-346. https://doi.org/10.12989/gae.2022.28.4.335.

Zhang, Y., Nian, T., Guo, X., Chen, G. and Zheng, L. (2019), "Modelling the flexural buckling failure of stratified rock slopes based on the multilayer beam model", *J. Mountain Sci.*, **16**, 1170-1183. https://doi.org/10.1007/s11629-018-5007-1.

Zhang, Z., Guo, Y., Dai, F., Zhao, S. and Yao, A. (2022), "Analysis of buckling failure process for the Xiaguiwa landslide in southeastern Tibetan Plateau", *Q J Eng Geol Hydrogeol*, **53**(3), 37-47. https://doi.org/10.1144/qjegh2021-075.

Zhao, S., Chigira M. and Wu, X. (2018), "Buckling deformations at the 2017 Xinmo landslide site and nearby slopes, Maoxian, Sichuan, China", *Eng. Geol.*, **246**, 187-197. https://doi.org/10.1016/j.enggeo.2018.09.033.

GC